Review

Assessment of EMF Troubles of Biological and Instrumental Medical Questions and Analysis of Their Compliance with Standards

Adel Razek

Group of Electrical Engineering—Paris (GeePs), French National Centre for Scientific Research (CNRS), University of Paris-Saclay and Sorbonne University, F91190 Gif sur Yvette, France; adel.razek@centralesupelec.fr

Abstract: This contribution aims to analyze compliance with the rules relating to disturbances in the domain of health due to exposure to electromagnetic fields (EMF). This concerns safety standards for exposed living tissue and the integrity of exposed medical devices acting on the body. This investigation is carried out by reviewing and analyzing these exposure effects. In the paper, the EMF exposure, the nature of sources and the characters of their interactions with objects are first illustrated. Then, EMF exposure restrictions accounting for living tissues safety standards as well as medical devices constancy are discussed. Exposure biological effects comprising both thermal and non-thermal effects are then detailed. The verification and control of EMF effects are next illustrated including mathematical modeling of EMF effects, governing equations and body tissues representation in the solution of these equations. At the end of the paper, two examples representing the cases of tissues and devices are given to check the rules under exposure to EMF: biological effects on exposed human tissues and integrity of a magnetic resonance imager under external disturbance.

Keywords: EMF exposure; safety standards; medical device integrity; compliance verification; living tissues; mathematical modeling

1. Introduction

Through the growth in the exercise of electromagnetic fields (EMF) in everyday life, various investigation works concerning their consequences have been dedicated in different domains. One of the most significant concerns is in the health domain. Studies have focused on the effects of electromagnetic (EM) sources on humans and health care devices. Two questions generally guide assessments of the effects of exposure to electromagnetic fields. The first is to assess induced fields in the tissues and physical consequences to assess possible health effects according to international safety standards [1–3]. The second challenge is to assess the risk of disruption of medical devices, integrated or associated with the body, used in therapy or involved in interventions.

Concerning the body tissues' exposure to the EMF atmosphere, the international health safety standards relative to exposure to external EMF are an established function with different parameters. These include, furthermore to the field characters (strength and frequency) and the interval, the tissue density and its physical properties. Such properties hang on the fragment of the tissue reflected and the class of the theme exposed along with the display conditions. These safety health standards fix limits connected to the effects of exposure to EMF accounting for the mentioned parameters. Regarding the emitted EMF, typically the mainly involved devices are those exerting significant stray fields as wireless energy and signal transmission devices. These implicate wide spreads of power and frequency. Two important categories are involved: digital communication and wireless power transfer. The circumstances of telecommunications involve ordinary EMF sources—for instance, radiofrequency (RF) waves emitted by antennas, Wi-Fi points, smartphones, mobile phones and Bluetooth tools. As the expended frequencies are high, and the exposed

item regards the body tissues, controlling their safety conditions is necessary; see, e.g., [4–9]. In the case of wireless charging systems, applications vary from small devices such as telephone sets to high-powered devices, such as electric vehicles (EV). Various works have been carried out concerning the analysis of safety in the case of low power; see, e.g., [10–13]. High power tools such as those discussed in [14–20] present solid nearby EMF and can yield large fields in the body tissues, and we must identify the situations in which the charging scheme can conform to security; see, e.g., [21–26]. Note that the effects of exposure to EMF are different in these two application categories. In that of wireless communication tools (WCT), the field asset is relatively modest, but the exploited frequency is great, and the part of the body exposed is mainly the head area. In such circumstance, the most important biological effect (BE) is concentrated on the brain. In the situation of wireless inductive power transfer (IPT), as in EV battery-charging systems, the field intensity may be strong and display high leakage; the frequency is small; and the exposure regards bodies near the device. In these conditions, BE concerns the initiation of EMFs in the body.

Concerning disturbances in the operation of medical devices, these are generally shielded against external fields to avoid disturbing the on-board electronics. Nevertheless, in the case of devices whose operation is based on electromagnetic fields that could be disturbed by external fields or objects involved in medical instruments near or inside the device, typical examples are static fixed-function wearable measuring tools—e.g., [27–29]— active organ stimulation tools—e.g., [30,31]—and magnetic resonance imagers (MRI) used in image-guided therapies and interventions. Actually, these image-guided operations can use several types of imagers, e.g., [32–38]. Among these imagers, only two are free of ionizing radiation: the MRI and ultrasound imager (USI) [34–38]. However, the USI can only work without air or bones. The MRI seems to be the best solution, but as mentioned before, it is subject to perturbation by external EMF or objects involved in medical instruments near or inside the imager. To control the integrity of the MRI, an analysis of electromagnetic compatibility (EMC) is needed [39–45]. In general, in all of the above-mentioned medical devices that are subject to disturbance by EMF, an EMC control is necessary to verify the integrity of the medical device against the external field.

In both the above-described situations of biological tissues and medical devices, the most effective means for verification of the external field effect seem to be numerical tools based on mathematical modeling of the equations involved. The subject modeled can be the tissue of the body part (represented by an equivalent phantom) or the structure of the part of the medical device concerned.

The methodology followed in this contribution concerns mainly such verification of external field effects. In both cases of tissues and devices, the electromagnetic model facilitates the estimates of local distributed fields allowing the verification of the field thresholds relative to the tissues as well as the EMC analysis in the devices. Moreover, in the case of tissues, the bio-thermal model connected to the electromagnetic model allows the calculation of the temperature rise to verify the thermal threshold in the tissues.

This contribution aims to analyze compliance with the standards relating to health domain troubles due to exposure to electromagnetic fields (EMF). This concerns the exposed living tissues of the body and the interaction with medical devices acting on the body. In the paper, first we give a description of EMF exposure involving the nature of sources and the characters of their interactions. Then we present EMF exposure restrictions accounting for living tissues' safety standards as well as medical devices constancy. Exposure biological effects will be detailed next including both thermal and non-thermal effects. This investigation will be carried out by reviewing and analyzing these exposure effects. Then, the verification and control of EMF effects will be illustrated including mathematical modeling of EMF effects, governing equations and tissues representation in these equations. At the end of the paper, we present two examples of cases of verifications: biological effects on exposed human tissues and EMC control in an MRI.

2. EMF Exposure

In different situations, EMFs are consumed every day in several sociable purposes. Additionally, they are employed securely in medical treatments. Conversely, when these fields are operated inadvertently, it can crop unfavorable outcomes. These consequences are intimately linked to the type of the EMF and the exposed substance. The strength of the field as well as its frequency typify EMF, whereas the physical and geometric properties describe matter.

2.1. Nature of EMF Sources

Essentially, the outcomes due to EMF exposure can be split into two different groups regarding the frequency ranges. One comprises the range of 10^3–10^{14} Hz for which waves can be divided into radio, microwaves and infrared that return non-ionizing radiation. The other interests the range of 10^{15}–10^{22} Hz divided into ultraviolet, X and gamma rays, which create ionizing radiation. It is likely in this case to have hostile health effects by creating tissue damage. EMFs of diverse frequencies, in the scale of non-ionizing class, function in numerous situations and still can disorder society.

In general, the emitting tools most involved in EMF non-ionizing exposure are, as mentioned before, those exercising noteworthy escaped fields such as wireless energy appliances including wide strength and frequency ranges. Two typical classes of such devices are WCT and IPT apparatuses. The case of WCT includes regular sources of RF, 10^5–$3.\,10^{11}$ Hz, while the case of IPT uses relatively low frequencies (less than 200 kHz).

2.2. Interactions of Sources and Living Tissues

In general, EMF sources can be divided into two classes: those working close to body tissues, producing an interacting near field greatly confined in a tissue portion of the body, and sources happening far away from the body that generate a total-body homogenous exposure. Roughly, far field relates to source-recipient distance superior to a wavelength, and its forte reduces quickly through distance. Interaction of the field with body tissues is influenced by the frequency, the field strength, the exposure time and the dielectric properties of absorbing matters. The character of interactions can produce effects due to short- or long-term exposure.

3. EMF Exposure Restrictions

Exposure to external sources of EMF can disrupt many societal domains. Health is a vital one in this concern. This affects living tissues in general and medical devices mainly when used in connection with living subjects.

3.1. Living Tissues Safety Standards

The health-safety standards fixed limits linking to tissue-specific absorption rate (SAR), subsequent temperature elevation and EMFs initiated in the living tissues. These thresholds account for the source specifications, the tissue properties and the exposure conditions and duration. These elements denote, on one hand, the part of the body considered that can be the head, trunk or limbs and the quality of the subject exposed that can be an adult, child or animal. On the other hand, they designate the exposure nature and duration for the different types of exposed persons (connected to the association with the source): employees concerned in fabrication, checking and settling devices, consumers using the tool and nearby items.

3.2. Medical Devices Constancy

Most of daily use devices are normally protected against external EMF exposure due to fabrication regulations of the emitting sources and the shielding of these exposed devices. Such protection concerns mainly the embedded electronics in these devices. The case of medical devices where the functioning is based on EMF and which are used nearby or on the body tissues is more complicated relative to the exposure to external EMF that can

perturb the device's self EMF. The complication can be augmented when using instruments employing EMF or involving materials perturbing fields nearby or inside the medical device. Typical examples are, as mentioned before, static fixed-function wearable sensing devices, active organ stimulation tools and MRI used in guided therapies and interventions. In these cases, as mentioned earlier, EMC analysis is necessary to verify the consistency of the medical device against the external field or perturbing materials.

4. Biological Effects of Exposure

Regarding BE, the case of exposure to great EMF (intensity and interval) can be hazardous to living tissues. Standards thresholds of induced EMF in the tissues can verify this. Such exposure may guide to tissue heating, in particular, for high frequencies (RF), causing heating that may provoke tissue harm. Two features reinforce such incidence. One links to the capacity of RF energy to quickly heat tissues. The other corresponds to the body's failure to endure the inconsistent temperature rise that can be created. Remark that the fragments of the tissues least defended from RF-EMF heating are those presenting deficiency in blood flow, which is the key method for dealing with severe heat. Note that disproportionate force fields can exhibit non-thermal effects.

4.1. Thermal Effects

The BE corresponding to thermal effect are related to the dissipation of electric power in living tissues. The density of this power per volume for conducting or dielectric materials is respectively given by

$$P_d = \sigma \cdot E^2/2 \qquad \text{low } \omega \text{ such that } \sigma >> \omega \cdot \varepsilon \qquad \text{mainly conductor} \qquad (1)$$

$$P_d = \omega \cdot \varepsilon'' \cdot E^2/2 \qquad \text{high } \omega \text{ such that } \sigma << \omega \cdot \varepsilon \qquad \text{mainly dielectric} \qquad (2)$$

The corresponding SAR is given by

$$SAR = P_d/\rho = \sigma \cdot E^2/(2\,\rho) \qquad \text{or} \qquad = \omega \cdot \varepsilon'' \cdot E^2/(2\,\rho) \qquad (3)$$

In (1–3), the parameters are as follows: σ is the electric conductivity of the heated material; ε'' is the imaginary part of the complex permittivity of the absorbing material; and ρ is the material density. The variable ω is the angular frequency = $2\pi f$; f is the frequency (Hz) of the exciting EMF; and E is the absolute peak value of the electric field strength (V/m), P_d (W/m^3) and SAR (W/kg).

The power dissipation density given by (2) relates to foremost dielectric heating of EMF energy loss relative to RF; see the discussion (Section 8) for more details.

The SAR, Equation (3), which values the energy absorbed by an element of a matter, can quantify the thermal effect induced by exposure to EMF. If multiplied by the exposure interval, the SAR signifies the specific absorbed energy amount. This energy generates a rise in matter temperature.

Generally, the quantity of heat absorbed by a lossy dielectric can be given as

$$\Delta Q = c\,m\,\Delta T \qquad (4)$$

where Q is the heat energy absorbed or dissipated in joule (J); m is the mass of the substance (kg); ΔT is the change in substance temperature (°C); c is the specific heat of the substance (the heat required to change a substance unit mass by one degree) in J/(kg·°C).

The power absorbed per unit mass of substance exposed to EMF, SAR (W/kg), which corresponds to the time derivative of the energy (J) absorbed per unit mass (kg) of substance can be given for an exposure time Δt (s) by

$$SAR = \Delta Q/(m \cdot \Delta t) = c \cdot \Delta T/\Delta t = \quad \sigma. E^2/(2\,\rho) \quad \text{or} \quad = \omega \cdot \varepsilon'' \cdot E^2/(2 \cdot \rho) \qquad (5)$$

Expression (5) implies that SAR value of substance varies with the induced electric field intensity, the exposure interval and the matter electrical-thermal properties. The energy absorbed by the substance is converted to thermal energy, triggering an increase in the temperature.

The temperature increase ΔT due to power dissipated by an electric field interacting with a lossy dielectric material specimen given for an exposure time Δt is obtained from (5):

$$\Delta T = \omega \cdot \varepsilon'' \cdot E^2. \ \Delta t/(2 \cdot c \cdot \rho) \qquad (6)$$

Note that Equation (6) gives the temperature rise in an element of a dielectric. For a living tissue, the heat transfer is usually represented by Penne's bio-heat equation [46] as is shown in Section 6.

4.2. Non-Thermal Effects

Apart from thermal effects, other types of interactions of RF EMF sources and tissues can also be more intricate, creating non-thermal effects relating various biochemical or bioelectrical concerns that affect cellular, molecular and chemical arrangements in living tissues [47–58]. These effects can be developed due to long-standing exposures or excessive short-range exposure involving high SAR values.

5. Verification and Control of EMF Effects

EMF effects on biological tissues and medical devices must be verified and controlled. The most effective means for accomplishing such a task is the use of numerical tools based on mathematical modeling. The electromagnetic model allows procurement of local distributed fields permitting the verification of the field thresholds relative to the tissues as well as the control by EMC analysis in the devices. The verification of thermal threshold in tissues can be accomplished by the computation of the local distribution of the temperature. This can performed through the bio-thermal model connected to the electromagnetic model.

6. Mathematical Modeling of EMF Effects

The evaluation of EMF effects can be performed through mathematical modeling of the EMF equations and the bio-heat tissue equation [46]. These governing equations can be locally solved in the object or tissues related to the effects. This can be achieved by means of numerical discretized techniques or other means permitting local calculations; see, e.g., [59–65].

6.1. Governing Equations

In the mentioned governing equations, the junction between EMF and heat equations is P_d or SAR, which can be obtained from EMF equations and used as input to the heat equation.

The EMF equations can be expressed as

$$\boldsymbol{\nabla} \times \mathbf{H} = \mathbf{J} \qquad (7)$$

$$\mathbf{J} = \sigma \, \mathbf{E} + j \, \omega \, \mathbf{D} + \mathbf{Je} \qquad (8)$$

$$\mathbf{E} = - \, \boldsymbol{\nabla} \, V - j \, \omega \, \mathbf{A} \qquad (9)$$

$$\mathbf{B} = \boldsymbol{\nabla} \times \mathbf{A} \qquad (10)$$

In the EMF Equations (7)–(10), $\mathbf{H}$ and $\mathbf{E}$ are the magnetic and electric fields; $\mathbf{B}$ and $\mathbf{D}$ are the magnetic and electric inductions; and $\mathbf{A}$ and V are the magnetic vector and electric scalar potentials. $\mathbf{J}$ and $\mathbf{J_e}$ are the total and source current densities; σ is the electric conductivity; and ω is the radial frequency pulsation. The symbol $\boldsymbol{\nabla}$ is a vector of partial derivative operators, and its three possible implications are gradient (product with a scalar

field), divergence and curl (dot and cross products, respectively, with a vector field). The magnetic and electric comportment laws between **B**/**H** and **D**/**E** are represented by the permeability μ and the permittivity ε, respectively.

Generally, in EM systems, the current is supplied by a voltage source across an external electric circuit. The next relation connecting the voltage v and the current i in the external circuit can be expressed as

$$v = 1/C. \int i \, dt + r \, i + L. \, di/dt + d\Psi/dt + \eth \tag{11}$$

In (11), r is the circuit resistance; L is a linear inductance; C is a capacitance; $\eth$ is a non-linear voltage drop (case of semiconductor component, e.g., a diode); and Ψ is the flux linkage in the coil.

The input source term in EM Equations (7)–(10) is $\mathbf{J_e}$ or its equivalent electric field σ $\mathbf{E_e}$. In case of IPT, the source $\mathbf{J_e}$ is related to "i" of Equation (11), and the EM equations to solve will be (7–11). In the case of WCT EMF exposure, the source will be $\sigma \, \mathbf{E_e}$, which corresponds to $\omega \, \varepsilon'' \, \mathbf{E_e}$ in living tissue, and the EM equations to solve will be (7–10).

P_d given by (1) or (2), depending on the material—respectively, conductor or dielectric— and SAR given by (3) can be determined from the solution of (7–10, 11).

The general heat transfer equation can be given by

$$c \, \rho \, \partial T/\partial t = \nabla \cdot (k \, \nabla T) + P_d + P_{conv} \tag{12}$$

The bio-heat tissue equation can be given by

$$c \, \rho \, \partial T/\partial t = \nabla \cdot (k \, \nabla T) + \rho \, (SAR) + q_{met} - c_b \, \rho_b \, \omega_b \, (T - T_b) \tag{13}$$

where P_{conv} is convective power density in (W/m^3); k is thermal conductivity; T is the local temperature in °C; q_{met} is the basal metabolic heat source in W/m^3; c_b is blood-specific heat in J/ (kg. °C); ρ_b is blood density in kg/m^3; ω_b is blood perfusion rate (1/s); T_b blood temperature in °C. $\nabla \cdot (k \, \nabla T)$ symbolizes heat equation in differential form; and $\rho \, (SAR)$ is the power density in (W/m^3) absorbed in the tissues.

6.2. Solution Approach

The solution of EMF Equations (7)–(11) permits us to calculate the provoked EMFs, for a given frequency, in the object or tissues. The SAR value as well as the EMC analysis checking the perturbations of devices (embedded or not) can be obtained from the values of these EMFs. Penne's bio-heat equation given by (13) permits us to determine heat transfer in living tissues. Thermal conduct in tissues due to exposure within the SAR is governed by Equations (2), (3), (7)–(10) and (13).

Concerning the solution of Equations (7)–(11) and (13) that correspond to EMF, external circuit and bio-thermal behaviors, note that the approach of solution depends on the relative values of time constants of the involved phenomena. When these time constants are near, the equations of concerned phenomena need to be solved through a strong (simultaneous) coupling; this is the case of EMF and external circuit equations. Opposing, with far time constants, the corresponding equations can be solved in a weak coupling manner (iteratively); this is the case of EMF and thermal equations; see, e.g., [66,67].

The equations can be solved in a coupled way (strong or weak) and locally (by discretized techniques) in the proper part of the device or the tissue. The obtained outputs are the local distributions in the device or the tissue of P_d, SAR, ΔT and produced EMFs.

6.3. Tissues Representation

In the practice of local computations of EMF in body tissues, we need suitable models of the body and ample data of the tissues properties at the actual frequency. These models are of homogeneous or non-homogeneous types. For the former, the dielectric properties of the tissues are regularly labeled as a 2/3 equivalent model [68]. For the other, layered

tissue, phantom models are attuned on data attained from MRI techniques, suggesting tissue shape accuracy in the order of mm [69]. Figure 1 shows an anatomical whole model of the body and its various details. Such a high-resolution tissue model is well suited with the approaches expended for the calculation of produced fields in human tissues. The dielectric possessions of tissues are extensively presented in [70].
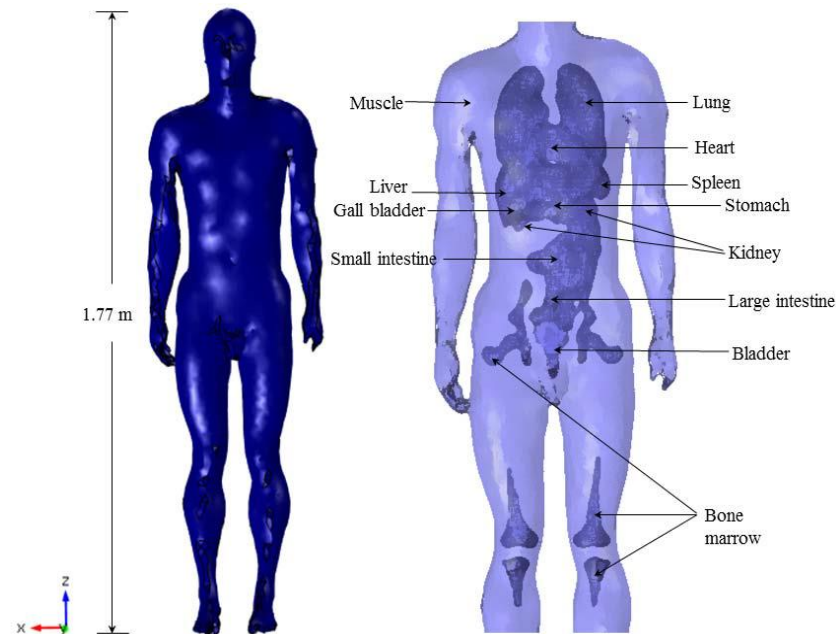

Figure 1. High-resolution anatomical entire body model and its diverse organs and tissues.

7. Cases of Verifications

In this section, two examples of standards or compatibility are verified through the approach explained in the last section. For this, we will consider the case of safety standard verification for an EMF exposure of a human body by an IPT and the control of the integrity of the RF field involved in a MRI under perturbation conditions due to the introduction of external matter in the imager.

7.1. Human-Induced EMFs due to Exposure to an IPT

In this section, we will consider the instance of EMF exposure of body tissues by IPT of EV battery charging system. As the used frequencies in this case are relatively low, the main important standard thresholds to verify are those of EMF induced in the tissues. Figure 2 displays an illustration of the induced fields distributions in human body tissues exposed to an IPT of EV. The modeled elements are the body (phantom) placed on the ground alongside the vehicle, the IPT coils, ferrites and the vehicle chassis [71,72]. The used human body phantom is the one shown in Figure 1, which is compatible with the employed numerical approach. The obtained results are in conformity with safety standards (27 μT for B and 4.05 V/m for E).
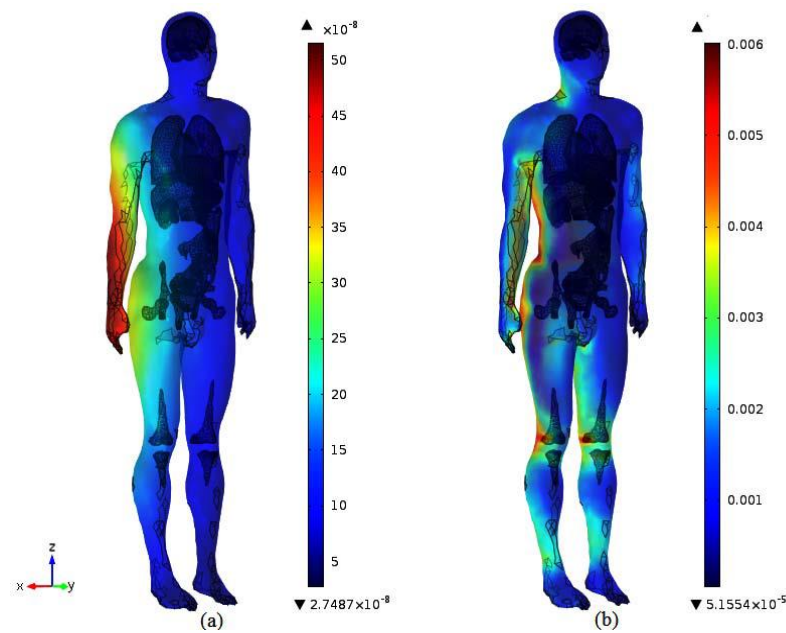
Figure 2. Provoked field distributions in a body exposed to an IPT below an EV, for a horizontal configuration, and ground placed body beside the EV. (**a**) B (T), (**b**) E (V/m) [71,72].

7.2. EMC Control in a MRI

In this section, we will consider the instance of disturbances in the MRI-involved RF magnetic field distribution inside its tunnel, which can generally be triggered by external EMF or the introduction of conductive or magnetic matters in the RF coil placed into the tunnel inside the imager. Both of these external intrusions, field or matter, have the same perturbation effect on the RF MRI field. Due to this, external fields are restricted, and only compatible matter can be introduced. One of the most efficient image-guided operation sets, as mentioned earlier, is the one using MRI. In MRI-guided interventions and therapies, only compatible devices and actuation tools constructed of materials which are not magnetic or conductive can be used. Piezoelectric material is ordinarily permitted, and actuators built of such material can normally be used [73–79]. In such actuation, we need electrodes (skinny conductive coverings) allowing the control of the piezoelectric. The checking of the disruption due to the insertion of different structures has been investigated in [71,72]. EMC analysis of different material structures indicated that only the conductive one is incompatible. Moreover, a simple configuration of piezo material layered with two electrodes of skinny layers was controlled by EMC examination. The two situations of electrodes perpendicular or parallel to the field direction have been examined. Figure 3 shows the MRI RF magnetic field distribution (vertically oriented) in the cross-section of the cage within the MRI tunnel for the no material reference case. In Figure 4, the case of piezoelectric material of cubic form ($\mu_r = 1$, $\varepsilon_r = [450,990,990]$, $\sigma = 0$ S/m) covered on two opposite faces by conductive tiny electrodes ($\mu_r = 1$, $\varepsilon_r = 1$, $\sigma = 3.77 \times 10^7$ S/m) is reflected (see Figure 4a). The figure displays the field distribution in the two situations of electrodes perpendicular (Figure 4b) and parallel (Figure 4c) to the field direction.

Remark that the piezoelectric almost does not perturb the field, and that the relative orientation of the fine conductive layers to the field acts a central role; this is due to the surface of the conductor facing the field direction. In Figure 4, it can be seen that only the electrodes perpendicular to the field perturb its distribution, and that the influence of conductive electrodes can be considerably diminished by putting them parallel to the field. Note that the distributions of Figures 3 and 4 are attained for identical source states; thus, they can give a behavioral suggestion. In addition, it is assumed that the other MRI fields are compensated and shielded. This EMC analysis in MRI illuminates a policy for monitoring any disorders during image-guided operations.
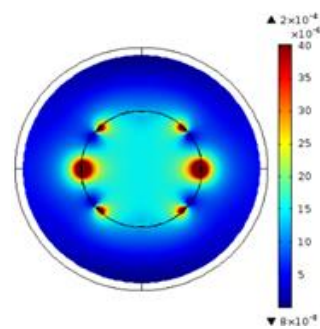
Figure 3. Distribution of the MRI RF magnetic field (vertically oriented) in the no material reference case within the MRI tunnel [71,72].
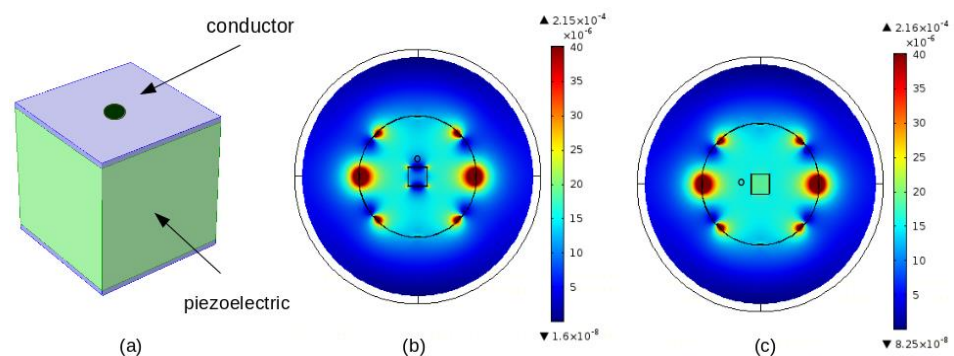

Figure 4. Distribution of the MRI RF magnetic field in the situation of insertion of a piezoelectric coated by electrodes (**a**) structure configuration, (**b**) distribution with electrodes perpendicular to the field, and (**c**) distribution with electrodes parallel to the field [71,72].

8. Discussion

In the present work, the investigation and analysis of the strategy of verification and control of compliance with the standards and rules relating to disturbances by EMF have displayed that such a strategy is valuable. This involved exposed body living tissues and the interaction with medical devices acting on the body. At this step, different arguments are valuable commenting on the following:

- As discussed in the paper, such strategy of verification and control can be centered on numerical tools based on mathematical models including EMF and bio-thermal governing equations. Such strategy is summarized in Figure 5, which illustrates schematics of the strategy. Inputs are source characters, object geometry and parameters, exposure interval and tissue physical parameters. Outputs are distributed fields of E, B, J, SAR and ΔT, which permit us to verify standards thresholds in tissues and to control devices integrity via EMC analysis.

- Concerning power dissipation densities, as conferred in the paper, we have noticed that such dissipation in conductor or dielectric matter depends on not only the physical proprieties of conductivity and permittivity of the matter but also on the EMF involved frequency. The two dissipation types are related to the relative values of the conductivity and the permittivity multiplied by the angular frequency (σ and $\omega.\varepsilon$). They are functions, respectively of σ and $\omega \cdot \varepsilon''$, where ε'' is the imaginary part of the permittivity ε that is frequency-dependent. It denotes the capacity of a dielectric to transform EMF energy into heat.

- Wide practice of wireless communication tools in one usage requires estimation exhibiting all these tools, taking into account the likely exposure effects of each. This combined devices situation requests a global SAR evaluation in the various tissues. This complex problem looks significant mainly if the frequencies of the sources are different. This problem could be grave in numerous real environments linked mainly to indoor instances such as therapeutic centers, shopping malls, etc. A future exploratory

challenge could be the establishment of a mathematical EM model relating 'n' diverse frequencies exclusive of doing 'n' successive solutions. This would be, in addition to disproportionate computations, incorrect due to ignoring the interactions of sources. Sole particular numeric extensions would solve this problematic issue.

- This contribution may be of interest to the various players involved in this subject, in particular the digital communication wireless energy systems industry, standardization authorities, medical staff, patients, the medical instruments and devices industry and researchers in various fields.
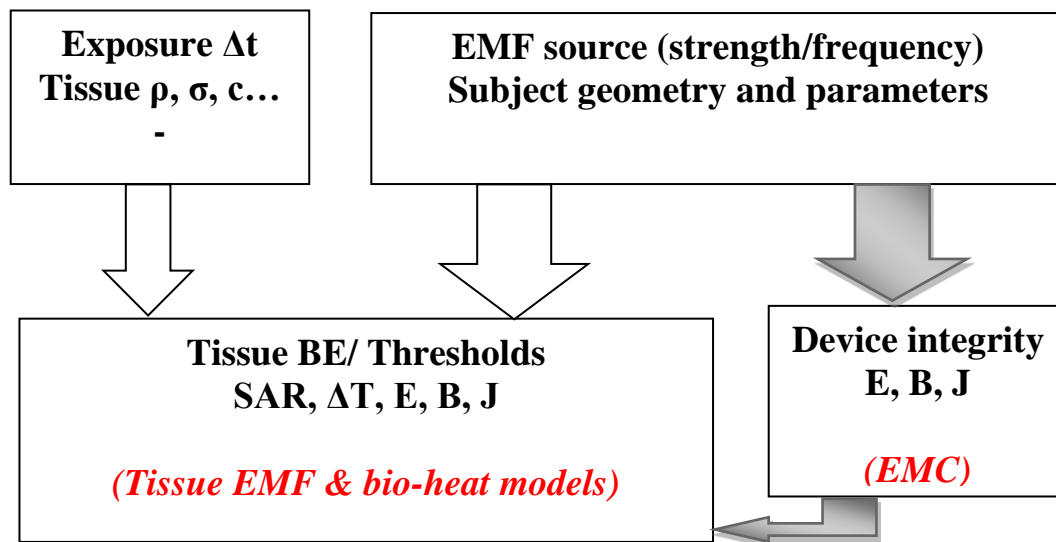
```
┌──────────────────────┐   ┌──────────────────────────────────────┐
│ Exposure Δt          │   │ EMF source (strength/frequency)       │
│ Tissue ρ, σ, c…      │   │ Subject geometry and parameters       │
│        -             │   │                                        │
└──────────────────────┘   └──────────────────────────────────────┘
         │                          │                    │
         ▼                          ▼                    ▼
┌───────────────────────────────────────────┐   ┌──────────────────┐
│      Tissue BE/ Thresholds                 │   │ Device integrity │
│      SAR, ΔT, E, B, J                      │   │ E, B, J          │
│                                            │   │                  │
│  (Tissue EMF & bio-heat models)            │◄──│   (EMC)          │
└───────────────────────────────────────────┘   └──────────────────┘
```

Figure 5. Schematics of the strategy verifying health-safety standard thresholds in body living tissues and device integrity due to interaction with EMF. Numerical used tools are indicated in red color.

9. Conclusions

The objectives of this paper were to analyze compliance with the standards relating to health domain troubles due to exposure to EMF. The following recapitulate the conclusion of the article:

- The compliance with the standards of the exposed living tissues of the body and rules relating to disturbances of medical devices acting on the body have been analyzed, illustrated and evaluated.
- Exposure biological effects including both thermal and non-thermal effects as well as interaction of EMF with medical devices have been illustrated and discussed.
- Verification and control of EMF effects have been demonstrated via mathematical modeling of EMF effects through their governing equations and illustrated in the two studied categories by two examples of cases of verifications: human tissues-induced EMF and EMC control in a MRI.
- A future investigative challenge would be the exposure mathematical model of combined sources with different frequencies.

Institutional Review Board Statement: Not applicable.

Informed Consent Statement: Not applicable.

Data Availability Statement: Not applicable.

Conflicts of Interest: The author declares no conflict of interest.

References

1. International Commission on Non-Ionizing Radiation Protection. Guidelines for limiting exposure to time-varying electric and magnetic fields for low frequencies (1 Hz–100 kHz). *Health Phys.* **2010**, *99*, 818–836. [CrossRef] [PubMed]
2. International Commission on Non-Ionizing Radiation Protection. Guidelines for limiting exposure to electromagnetic fields (100 kHz to 300 GHz). *Health Phys.* **2020**, *118*, 483–524. [CrossRef] [PubMed]
3. *C95.1-2019*; IEEE Standard for Safety Levels With Respect to Human Exposure to Electric, Magnetic, and Electromagnetic Fields, 0 Hz to 300 GHz. IEEE: Piscataway, NJ, USA, 2019. [CrossRef]
4. Joshi, M.S.; Joshi, G.R. Analysis of SAR induced in Human Head due to the exposure of Non-ionizing Radiation. *Int. J. Eng. Res. Technol. (IJERT)* **2016**, *5*, IJERTV5IS020466. [CrossRef]
5. Sallomi, A.H.; Hashim, S.A.; Wali, M.H. SAR and thermal effect prediction in human head exposed to cell phone radiations. *Sci. Int.* **2018**, *30*, 653–656. Available online: https://www.researchgate.net/publication/339415489 (accessed on 19 April 2023).
6. Hamed, T.; Maqsood, M. SAR Calculation & Temperature Response of Human Body Exposure to Electromagnetic Radiations at 28, 40 and 60 GHz mm Wave Frequencies. *Prog. Electromagn. Res. M* **2018**, *73*, 47–59. [CrossRef]
7. Baker-Jarvis, J.; Kim, S. The Interaction of Radio-Frequency Fields With Dielectric Materials at Macroscopic to Mesoscopic Scales. *J. Res. Natl. Inst. Stand. Technol.* **2012**, *117*, 1–60. [CrossRef]
8. Razek, A. Assessment and Categorization of Biological Effects and Atypical Symptoms Owing to Exposure to RF Fields from Wireless Energy Devices. *Appl. Sci.* **2023**, *13*, 1265. [CrossRef]
9. Bernardi, P.; Cavagnaro, M.; Pisa, S.; Piuzzi, E. Specific absorption rate and temperature elevation in a subject exposed in the far-field of radio-frequency sources operating in the 10–900-MHz range. *IEEE Trans. Biomed. Eng.* **2003**, *50*, 295–304. [CrossRef]
10. Okoniewski, M.; Stuchly, M.A. A study of the handset antenna and human body interaction. *IEEE Trans. Microw. Theory Tech.* **1996**, *44*, 1855–1864. [CrossRef]
11. Shiba, K.; Higaki, N. Analysis of SAR and Current Density in Human Tissue Surrounding an Energy Transmitting Coil for a Wireless Capsule Endoscope. In Proceedings of the 2009 20th International Zurich Symposium on Electromagnetic Compatibility, Zurich, Switzerland, 12–16 January 2009; pp. 321–324. [CrossRef]
12. Christ, A.; Douglas, M.G.; Roman, J.M.; Cooper, E.B.; Sample, A.P.; Waters, B.H.; Smith, J.R.; Kuster, N. Evaluation of wireless resonant power transfer systems with human electromagnetic exposure limits. *IEEE Trans. Electromagn. Compat.* **2013**, *55*, 265–274. [CrossRef]
13. Lin, J.C. Safety of Wireless Power Transfer. *IEEE Access* **2021**, *9*, 125342–125347. [CrossRef]
14. Covic, G.A.; Boys, J.T. Trends in Inductive Power Transfer for Transportation Applications. *IEEE J. Emerg. Sel. Top. Power Electron.* **2013**, *1*, 28–41. [CrossRef]
15. Hutchinson, L.; Waterson, B.; Anvari, B.; Naberezhnykh, D. Potential of wireless power transfer for dynamic charging of electric vehicles. *IET Intell. Transp. Syst.* **2019**, *13*, 3–12. [CrossRef]
16. Ibrahim, M.; Bernard, L.; Pichon, L.; Razek, A.; Houivet, J.; Cayol, O. Advanced modeling of a 2-kw series–series resonating inductive charger for real electric vehicle. *IEEE Trans. Veh. Technol.* **2015**, *64*, 421–430. [CrossRef]
17. Cirimele, V.; Diana, M.; Freschi, F.; Mitolo, M. Inductive Power Transfer for Automotive Applications: State-of-the-Art and Future Trends. *IEEE Trans. Ind. Appl.* **2018**, *54*, 4069–4079. [CrossRef]
18. Razek, A. Review of Contactless Energy Transfer Concept Applied to Inductive Power Transfer Systems in Electric Vehicles. *Appl. Sci.* **2021**, *11*, 3221. [CrossRef]
19. Ibrahim, M.; Bernard, L.; Pichon, L.; Laboure, E.; Razek, A.; Cayol, O.; Ladas, D.; Irving, J. Inductive Charger for Electric Vehicle: Advanced Modeling and Interoperability Analysis. *IEEE Trans. Power Electron.* **2016**, *31*, 8096–8114. [CrossRef]
20. Cirimele, V.; Diana, M.; Bellotti, F.; Berta, R.; El Sayed, N.; Kobeissi, A.; Guglielmi, P.; Ruffo, R.; Khalilian, M.; La Ganga, A.; et al. The Fabric ICT Platform for Managing Wireless Dynamic Charging Road Lanes. *IEEE Trans. Veh. Technol.* **2020**, *69*, 2501–2512. [CrossRef]
21. Ding, P.; Bernard, L.; Pichon, L.; Razek, A. Evaluation of Electromagnetic Fields in Human Body Exposed to Wireless Inductive Charging System. *IEEE Trans. Magn.* **2014**, *50*, 1037–1040. [CrossRef]
22. Wen, F.; Huang, X. Human Exposure to Electromagnetic Fields from Parallel Wireless Power Transfer Systems. *Int. J. Environ. Res. Public Health* **2017**, *14*, 157. [CrossRef]
23. Wang, Q.; Li, W.; Kang, J.; Wang, Y. Electromagnetic Safety Evaluation and Protection Methods for a Wireless Charging System in an Electric Vehicle. *IEEE Trans. Electromagn. Compat.* **2019**, *61*, 1913–1925. [CrossRef]
24. Cirimele, V.; Freschi, F.; Giaccone, L.; Pichon, L.; Repetto, M. Human Exposure Assessment in Dynamic Inductive Power Transfer for Automotive Applications. *IEEE Trans. Magn.* **2017**, *53*, 5000304. [CrossRef]
25. Park, S. Evaluation of Electromagnetic Exposure During 85 kHz Wireless Power Transfer for Electric Vehicles. *IEEE Trans. Magn.* **2018**, *54*, 5100208. [CrossRef]
26. Asa, E.; Mohammad, M.; Onar, O.C.; Pries, J.; Galigekere, V.; Su, G.-J. Review of Safety and Exposure Limits of Electromagnetic Fields (EMF) in Wireless Electric Vehicle Charging (WEVC) Applications. In Proceedings of the 2020 IEEE Transportation Electrification Conference & Expo (ITEC) 2020, Chicago, IL, USA, 23–26 June 2020; pp. 17–24. [CrossRef]
27. Guk, K.; Han, G.; Lim, J.; Jeong, K.; Kang, T.; Lim, E.-K.; Jung, J. Evolution of Wearable Devices with Real-Time Disease Monitoring for Personalized Healthcare. *Nanomaterials* **2019**, *9*, 813. [CrossRef] [PubMed]

28. Xin, Y.; Liu, T.; Sun, H.; Xu, Y.; Zhu, J.; Qian, C.; Lin, T. Recent progress on the wearable devices based on piezoelectric sensors. *Ferroelectrics* **2018**, *531*, 102–113. [CrossRef]

29. Yetisen, A.K.; Martinez-Hurtado, J.L.; Ünal, B.; Khademhosseini, A.; Butt, H. Wearables in Medicine. *Adv. Mater.* **2018**, *30*, 1706910. [CrossRef]

30. Bernardi, P.; Cavagnaro, M.; Pisa, S.; Piuzzi, E. Safety Aspects of Magnetic Resonance Imaging for Pacemaker Holders. In Proceedings of the 2009 International Conference on Electromagnetics in Advanced Applications 2009, Turin, Italy, 14–18 September 2009; pp. 869–872. [CrossRef]

31. Thotahewa, K.M.S.; Redouté, J.; Yuce, M.R. Electromagnetic and Thermal Effects of IR-UWB Wireless Implant Systems on the Human Head. In Proceedings of the 2013 35th Annual International Conference of the IEEE Engineering in Medicine and Biology Society (EMBC), Osaka, Japan, 3–7 July 2013; pp. 5179–5182. [CrossRef]

32. Kovács, A.; Bischoff, P.; Haddad, H.; Kovács, G.; Schaefer, A.; Zhou, W.; Pinkawa, M. Personalized Image-Guided Therapies for Local Malignencies: Interdisciplinary Options for Interventional Radiology and Interventional Radiotherapy. *Front. Oncol.* **2021**, *11*, 616058. Available online: https://www.frontiersin.org/article/10.3389/fonc.2021 (accessed on 19 April 2023). [CrossRef]

33. Zhao, J.; Zhi, Z.; Zhang, H.; Zhao, J.; Di, Y.; Xu, K.; Ma, C.; Liu, Z.; Sui, A.; Wang, J. Efficacy and safety of CT guided 125I brachytherapy in elderly patients with non small cell lung cancer. *Oncol. Lett.* **2020**, *20*, 183–192. [CrossRef]

34. Park, B.K. Ultrasound-guided genitourinary interventions: Principles and techniques (Review Article). *Ultrasonography* **2017**, *36*, 336–348. [CrossRef]

35. Pinto, P.A.; Chung, P.H.; Rastinehad, A.R.; Baccala, A.A., Jr.; Kruecker, J.; Benjamin, C.J.; Xu, S.; Yan, P.; Kadoury, S.; Chua, C.; et al. Magnetic resonance imaging/ultrasound fusion guided prostate biopsy improves cancer detection following transrectal ultrasound biopsy and correlates with multiparametric magnetic resonance imaging. *J. Urol.* **2011**, *186*, 1281–1285. [CrossRef]

36. Fiard, G.; Hohn, N.; Descotes, J.L.; Rambeaud, J.J.; Troccaz, J.; Long, J.A. Targeted MRI-guided prostate biopsies for the detection of prostate cancer: Initial clinical experience with real-time 3-dimensional transrectal ultrasound guidance and magnetic resonance/transrectal ultrasound image fusion. *Urology* **2013**, *81*, 1372–1378. [CrossRef]

37. Veltri, A.; Garetto, I.; Pagano, E.; Tosetti, I.; Sacchetto, P.; Fava, C. Percutaneous RF thermal ablation of renal tumors: Is US guidance really less favorable than other imaging guidance techniques? *Cardiovasc. Intervent. Radiol.* **2009**, *32*, 76–85. [CrossRef] [PubMed]

38. Bassignani, M.; Moore, Y.; Watson, L.; Theodorescu, D. Pilot experience with real-time ultrasound guided percutaneous renal mass cryoablation. *J. Urol.* **2004**, *171*, 1620–1623. [CrossRef] [PubMed]

39. Chinzei, K.; Kikinis, R.; Jolesz, F.A. MR Compatibility of Mechatronic Devices: Design Criteria. In Proceedings of the Medical Image Computing and Computer-Assisted Intervention—MICCAI'99, Cambridge, UK, 19–22 September 1999; pp. 1020–1030.

40. Tsekos, N.V.; Khanicheh, A.; Christoforou, E.; Mavroidis, C. Magnetic resonance-compatible robotic and mechatronics systems for image guided interventions and rehabilitation: A Review Study. *Annu. Rev. Biomed. Eng.* **2007**, *9*, 351–387. [CrossRef]

41. Khairi, R.; Razek, A.; Bernard, L.; Corcolle, R.; Bernard, Y.; Pichon, L.; Poirier-Quinot, M.; Ginefri, J.C. EMC analysis of MRI environment in view of Optimized performance and cost of image guided interventions. *Int. Jour. App. Electromag. Mech.* **2016**, *51*, S67–S74. [CrossRef]

42. Boutry, C. Biodegradable passive resonant circuits for wireless implant applications. DSc Dissertation, ETH Zurich, Zurich, Switzerland, 2012.

43. Razek, A. Towards an image-guided restricted drug release in friendly implanted therapeutics. *Eur. Phys. J. Appl. Phys.* **2018**, *82*, 31401. [CrossRef]

44. Hsu, Y.H.; Chen, D.W.; Tai, C.D.; Chou, Y.C.; Liu, S.J.; Ueng, S.W.; Chan, E.C. Biodegradable drug-eluting nanofiber-enveloped implants for sustained release of high bactericidal concentrations of vancomycin and ceftazidime: In vitro and in vivo studies. *Int. J. Nanomed.* **2014**, *9*, 4347–4355. [CrossRef]

45. Razek, A. Assessment of Supervised Drug Release in Cordial Embedded Therapeutics. *Athens J. Technol. Eng.* **2019**, *6*, 77–91. [CrossRef]

46. Pennes, H.H. Analysis of tissue and arterial blood temperatures in the resting human forearm. *J. Appl. Physiol.* **1998**, *85*, 5–34. [CrossRef]

47. Ramos, V.; Suarez, O.J.; Febles-Santana, V.M.; Suarez-Rodriguez, D.S.; Aguirre, E.; De-Miguel-Bilbao, S.; Marina, P.; Rabassa-Lopez-Calleja, L.E.; Celaya-Echarri, M.; Falcone, F.; et al. Electromagnetic Characterization of UHF-RFID Fixed Reader in Healthcare Centers Related to the Personal and Labor Health. *IEEE Access* **2022**, *10*, 28614–28630. [CrossRef]

48. Kim, J.H.; Lee, J.-K.; Kim, H.-G.; Kim, K.-B.; Kim, H.R. Possible effects of radiofrequency electromagnetic field exposure on central nerve system. *Biomol. Ther.* **2019**, *27*, 265–275. [CrossRef] [PubMed]

49. Scientific Committee on Emerging and Newly Identified Health Risks. *Opinion on Potential Health Effects of Exposure to Electromagnetic Fields (EMF)*; European Commission: Luxembourg, 2015; Available online: http://ec.europa.eu/health/sites/health/files/scientific_committees/emerging/docs/scenihr_o_041.pdf (accessed on 19 April 2023).

50. Sánchez-Hernández, D.A. *High Frequency Electromagnetic Dosimetry*; Artech House, Inc.: Norwood, MA, USA, 2009; ISBN 978-1-59693-397-2.

51. Wust, P.; Kortüm, B.; Strauss, U.; Nadobny, J.; Zschaeck, S.; Beck, M.; Stein, U.; Ghadjar, P. Non-thermal effects of radiofrequency electromagnetic fields. *Sci. Rep.* **2020**, *10*, 13488. [CrossRef] [PubMed]

52. Zradziński, P.; Karpowicz, J.; Gryz, K. Electromagnetic energy absorption in a head approaching a radiofrequency identification (RFID) reader operating at 13.56 MHz in users of hearing implants versus non-users. *Sensors* **2019**, *19*, 3724. [CrossRef]

53. Jalilian, H.; Eeftens, M.; Ziaei, M.; Röösli, M. Public exposure to radiofrequency electromagnetic fields in everyday microenvironments: An updated systematic review for Europe. *Environ. Res.* **2019**, *176*, 108517. [CrossRef] [PubMed]

54. Leach, V.; Weller, S.; Redmayne, M. A novel database of bio-effects from non-ionizing radiation. *Rev. Environ. Health* **2018**, *33*, 273–280. [CrossRef] [PubMed]

55. Dürrenberger, G.; Fröhlich, J.; Röösli, M.; Mattsson, M.-O. EMF monitoring—Concepts, activities, gaps and options. *Int. J. Environ. Res. Public Health* **2014**, *11*, 9460–9479. [CrossRef]

56. Röösli, M.; Frei, P.; Bolte, J.; Neubauer, G.; Cardis, E.; Feychting, M.; Gajsek, P.; Heinrich, S.; Joseph, W.; Mann, S.; et al. Conduct of a personal radiofrequency electromagnetic field measurement study: Proposed study protocol. *Environ. Health* **2010**, *9*, 9–23. [CrossRef]

57. Review of Published Literature between 2008 and 2018 of Relevance to Radiofrequency Radiation and Cancer. U.S. Food & Drug Administration 2020. Available online: https://www.fda.gov/media/135043/download (accessed on 19 April 2023).

58. World Cancer Report 2020—Cancer Research for Cancer Prevention, IARC/OMS, Lyon, France, 2020. Available online: https://www.aws.iarc.who.int/featured-news/new-world-cancer-report (accessed on 19 April 2023).

59. Wang, R.-Y.; Ding, P.-P. Electromagnetic Influence on Electric Vehicles by Wireless Inductive Charging System. In Proceedings of the 2019 International Conference on Microwave and Millimeter Wave Technology (ICMMT), Guangzhou, China, 19–22 May 2013; pp. 1–3. [CrossRef]

60. Krasopoulos, C.T.; Ioannidis, A.S.; Kremmydas, A.F.; Karafyllakis, I.A.; Kladas, A.G. Convection Heat Transfer Coefficient Regression Models Construction for Fast High-Speed Motor Thermal Analysis. *IEEE Trans. Magn.* **2022**, *58*, 8206905. [CrossRef]

61. Li, C.; Ren, Z.; Razek, A. An approach to adaptive mesh refinement for three-dimensional eddy-current computations. *IEEE Trans. Magn.* **1994**, *30*, 113–117. [CrossRef]

62. Nunes, A.S.; Dular, P.; Chadebec, O.; Kuo-Peng, P. Subproblems Applied to a 3-D Magnetostatic Facet FEM Formulation. *IEEE Trans. Magn.* **2018**, *54*, 7402209. [CrossRef]

63. Ren, Z.; Razek, A. New technique for solving three-dimensional multiply connected eddy-current problems. *IEEE Proc. 693 A Phys. Sci. Meas. Instr.* **1990**, *137*, 135–140. [CrossRef]

64. Arbab, N.; Wang, W.; Lin, C.; Hearron, J.; Fahimi, B. Thermal Modeling and Analysis of a Double-Stator Switched Reluctance Motor. *IEEE Trans. Energy Convers.* **2015**, *30*, 1209–1217. [CrossRef]

65. Sun, Q.; Zhang, R.; Zhan, Q.; Liu, Q.H. 3-D Implicit–Explicit Hybrid Finite Difference/Spectral Element/Finite Element Time Domain Method without a Buffer Zone. *IEEE Trans. Antennas Propag.* **2019**, *67*, 5469–5476. [CrossRef]

66. Razek, A. Coupled Models in Electromagnetic and Energy Conversion Systems from Smart Theories Paradigm to That of Complex Events: A Review. *Appl. Sci.* **2022**, *12*, 4675. [CrossRef]

67. Sekkak, A.; Pichon, L.; Razek, A. 3-D FEM magneto-thermal analysis in microwave ovens. *IEEE Trans. Magn.* **1994**, *30*, 3347–3350. [CrossRef]

68. Harris, L.R.; Zhadobov, M.; Chahat, N.; Sauleau, R. Electromagnetic Dosimetry for Adult and Child Models within a Car: Multi-Exposure Scenarios. *Int. J. Microw. Wirel. Technol.* **2011**, *3*, 707–715. [CrossRef]

69. Barchanski, A.; Steiner, T.; De Gersem, H.; Clemens, M.; Weiland, T. Local Grid Refinement for low-Frequency Current Computations in 3-D Human Anatomy Models. *IEEE Trans. Magn.* **2006**, *42*, 1371–1374. [CrossRef]

70. Gabriel, C.; Gabriel, S.; Corthout, E. The Dielectric Properties of Biological Tissues: II. Measurements in the Frequency Range 10 Hz to 20 GHz. *Phys. Med. Biol.* **1996**, *41*, 2251–2269. [CrossRef]

71. Razek, A.; Pichon, L.; Kameni, A.; Makong, L.; Rasm, S. Evaluation of Human Exposure owing to Wireless Power Transfer Systems in Electric Vehicles. *Athens J. Technol. Eng.* **2019**, *6*, 239–258. [CrossRef]

72. Razek, A. Biological and Medical Disturbances Due to Exposure to Fields Emitted by Electromagnetic Energy Devices—A Review. *Energies* **2022**, *15*, 4455. [CrossRef]

73. Hariri, H.; Bernard, Y.; Razek, A. A traveling wave piezoelectric beam robot. *Smart Mater. Struct.* **2014**, *23*, 025013. [CrossRef]

74. Lemaire, E.; Moser, R.; Borsa, C.J.; Shea, H.; Briand, D. Green paper-based piezoelectric material for sensors and actuators. *Procedia Eng.* **2015**, *120*, 360–363. [CrossRef]

75. Hariri, H.; Bernard, Y.; Razek, A. 2-D Traveling Wave Driven Piezoelectric Plate Robot for Planar Motion. *IEEE/ASME Trans. Mechatron.* **2018**, *23*, 242–251. [CrossRef]

76. Khan, A.; Abas, Z.; Kim, H.S.; Kim, J. Recent progress on cellulose-based electro-active paper, its hybrid nanocomposites and applications. *Sensors* **2016**, *16*, 1172. [CrossRef]

77. Dagdeviren, C.; Joe, P.; Tuzman, O.L.; Park, K.I.; Lee, K.J.; Shi, Y.; Huang, Y.; Rogers, J.A. Recent progress in flexible and stretchable piezoelectric devices for mechanical energy harvesting sensing and actuation. *Extrem. Mech. Lett.* **2016**, *9*, 269–281. [CrossRef]

78. Stapleton, A.; Noor, M.R.; Sweeney, J.; Casey, V.; Kholkin, A.L.; Silien, C.; Gandhi, A.A.; Soulimane, T.; Tofail, S.A.M. The direct piezoelectric effect in the globular protein lysozyme. *Appl. Phys. Lett.* **2017**, *111*, 142902. [CrossRef]

79. Su, Q.; Quan, Q.; Deng, J.; Yu, H. A quadruped micro-robot based on piezoelectric driving. *Sensors* **2018**, *18*, 810. [CrossRef]